coatings

MDPI

Article

First Principles Study of Gas Molecules Adsorption on Monolayered β-SnSe

Tianhan Liu [1], Hongbo Qin [1,*], Daoguo Yang [1] and Guoqi Zhang [1,2]

[1] School of Mechanical and Electronic Engineering, Guilin University of Electronic Technology, Guilin 541004, China; 1801302029@mails.guet.edu.cn (T.L.); d.g.yang@guet.edu.cn (D.Y.); g.q.zhang@tudelft.nl (G.Z.)

[2] EEMCS Faculty, Delft University of Technology, 2628 Delft, The Netherlands

* Correspondence: qinhb@guet.edu.cn; Tel.: +86-773-2290108

Received: 30 April 2019; Accepted: 13 June 2019; Published: 17 June 2019

Abstract: For the purpose of exploring the application of two-dimensional (2D) material in the field of gas sensors, the adsorption properties of gas molecules, CO, CO_2, CH_2O, O_2, NO_2, and SO_2 on the surface of monolayered tin selenium in β phase (β-SnSe) has been researched by first principles calculation based on density functional theory (DFT). The results indicate that β-SnSe sheet presents weak physisorption for CO and CO_2 molecules with small adsorption energy and charge transfers, which show that a β-SnSe sheet is not suitable for sensing CO and CO_2. The adsorption behavior of CH_2O molecules adsorbed on a β-SnSe monolayer is stronger than that of CO and CO_2, revealing that the β-SnSe layer can be applied to detect CH_2O as physical sensor. Additionally, O_2, NO_2, and SO_2 are chemically adsorbed on a β-SnSe monolayer with moderate adsorption energy and considerable charge transfers. All related calculations reveal that β-SnSe has a potential application in detecting and catalyzing O_2, NO_2, and SO_2 molecules.

Keywords: β-SnSe; first principles; gas sensor; gas molecules; adsorption behavior

1. Introduction

The detection of gases, especially the toxic gases, has aroused tremendous interest for its extensive application in the fields of agricultural production, industrial control, medical diagnosis, and environmental detection [1]. The traditional gas sensors, transition metal oxides sensors, have the shortcoming of a high operating temperature (200–600 °C) [2,3] and low sensing response [4], which have motivated researchers to search for appropriate materials as reliable and high performance gas sensors [5]. Fortunately, because 2D materials exhibit excellent physicochemical properties, such as the high ratio of surface area to volume [6], ultrahigh carrier mobility [7], excellent mechanical performance [8], and low electrical noise [9,10], it is possible for them to sense gas molecules at room temperature and normal pressure [11,12]. Within 2D materials, monolayered graphene has been immensely researched due to its commendable properties [13]. However, the lack of an energy band gap limits its applications in the fields of field-effect transistors, gas sensors, and computer chips [14,15]. On the contrary, some 2D materials have a large band gap, but they are unstable in air, such as silicene [16] and phosphorenes [17], which hinders their commercial applications. It is noteworthy that some stable layered materials also show semiconductor characteristics with an appropriate band gap, which is of vital importance for the sensing performance [18,19].

In addition, due to the low cost, rich elements, and environmental friendliness, 2D IV-VI semiconductors have become a research hotspot in recent years. Monolayered SnSe is a fascinating 2D material due to its ideal electric and thermal properties in the field of nanoelectronics [20], which means it has promising applications in the photovoltaic industry, cut-off devices, and infrared lasers [21–23]. It has been reported that the adsorption behaviors of some small gas molecules on a GeS sheet [11],

a SnS sheet [24], and an α-SnSe sheet [25]. Significatively, there are some reports pointing out that monolayered SnSe allotropes also show high thermoelectric performance, chemical stability, no toxicity, and earth abundance, which indicate that these monolayer SnSe allotropes can have a potential application in the field of next generation nano-photovoltaic devices and 2D optoelectronic material [15,26]. However, reports about the adsorption behaviors of β-SnSe for small gas molecules is scarce. Therefore, in this paper, the sensing behaviors of small gas molecules (CO, CO_2, CH_2O, O_2, NO_2, and SO_2) on a β-SnSe sheet were investigated by first principles calculation.

2. Materials and Methods

In this work, all the simulation calculations are presented by applying the DMOL^3 module in the Materials Studio [27]. Due to the fact that the conventional generalized gradient approximation (GGA) methods are inclined to underestimate the adsorption energy [14], the Perdew–Burke–Ernzerhof (PBE) of generalized gradient approximation (GGA) was applied as the exchange-correlation functional in the process of structural optimization [28], which is widely employed for its precision and economy [29]. Due to the existence of the tiny van der Waals interaction, the Grimme custom method for DFT-D correction was applied [30]. Moreover, the double numerical plus d-function (DND) basis set was carried out to achieve high computational quality of the density functional theory (DFT) calculation. It has been verified that the basic set superposition error (BSSE) effect is not considered when the numerical basis sets are applied in DMOL^3 [31–33]. For both geometric optimization and electronic properties calculations, the 4 × 4 × 1 Monkhorst–Pack k-point mesh was chosen. Considering the interaction between β-SnSe sheets of adjacent supercells, a 4 × 4 single-layered β-SnSe supercell with a vacuum region of 15 Å in the Z direction was utilized in the simulated system. Non-spin polarization was proposed in the investigation of the adsorbing properties, but not the two types of molecules (NO_2 and O_2) as they are paramagnetic [14]. In addition, all the correlation simulation calculations were completely performed until the displacement, energy, and force were converged to 0.005 Å, 0.002 Ha/Å (1 Ha = 27.21 eV), and 1×10^{-5} Ha, respectively.

Considering the different adsorption effects for the different initial configurations of SnSe toward the gas molecules, eight different adsorption initial locations for each molecule were calculated. On the Sn atoms side of β-SnSe layer, four adsorption sites were calculated, the T_1 point is located on top of the Sn atom, the T_2 point is located on top of the Se atom, the T_3 point is located in the middle of the Se–Sn bond, and the T_4 point is located in the center of the puckered hexagon. There are four equal configurations (T_5, T_6, T_7, T_8) on the Se atoms side of β-SnSe sheet, as shown in Figure 1. The initial distance of 3 Å is applied as the height of the gas molecules on top of the β-SnSe monolayer.

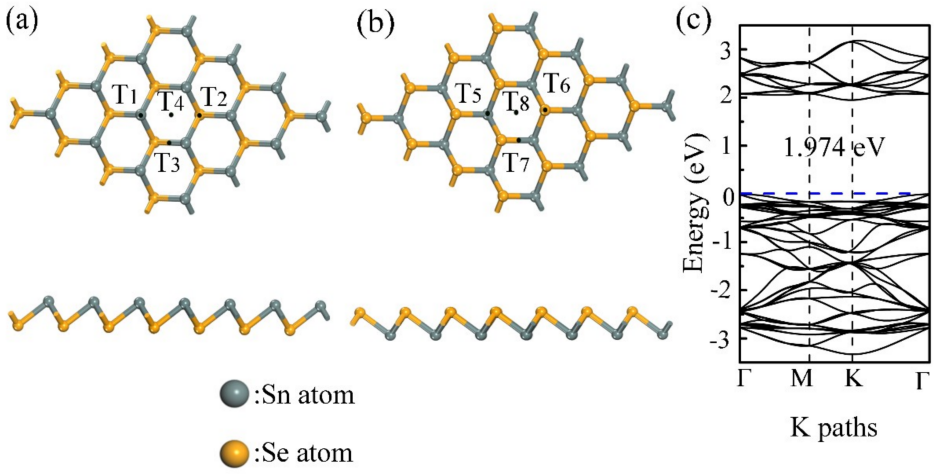

Figure 1. (**a**) Structure and initial adsorption sites of the Sn atom's side of the β-SnSe monolayer are presented in the picture; (**b**) structure and initial adsorption sites of the Se atom's side of the β-SnSe monolayer are presented in the picture, and (**c**) the band structure of the β-SnSe monolayer is shown in the picture.

For the purpose of intuitively accessing the adsorbing performance of the gas molecules adsorbed on the β-SnSe layer, we calculated the adsorption energy (E_a), the Hirshfeld charge transfer (Q_c), and the equilibrium distance (d_i). The negative value of Q_c expresses that gas molecules acquire charge from the β-SnSe layer, and the d_i stands for the balanced minimum distance between gas molecules and the β-SnSe layer. E_a is defined as follows:

$$E_a = E_{(\text{molecules + SnSe})} - E_{\text{SnSe}} - E_{\text{molecules}} \quad (1)$$

where $E_{(\text{molecules + SnSe})}$, E_{SnSe}, and $E_{\text{molecules}}$ denote the total energy of gas molecules on the SnSe sheet, a SnSe sheet, and a single gas molecule, respectively.

3. Results and Discussion

The lattice dimensions of the optimized 4 × 4 supercell structure are $a = b = 15.125$ Å, and the unit cell has a lattice constant of $a = b = 3.187$ Å. The parameters of structural optimizations are in accordance with the results in the previous work [26]. Additionally, a SnSe monolayer in β-phase is a semiconductor with a 1.974 eV band gap in the PBE method, which has a larger band gap than that of SnSe in α-phase (the band gap values of α-SnSe are 0.90 eV indirect and 1.30 eV direct) [15,26]. Judging from the result of the DFT calculation, the most stable sites of structural optimizations for gas molecules on the β-SnSe layer are presented in Figure 2. In addition, the adsorption parameters of the gas molecules adsorbed on the β-SnSe layer, such as E_a, d_i, and Q_c, are shown in Table 1. The E_a values of the CO, CO_2, and CH_2O gas molecules adsorbed on the β-SnSe monolayer are −0.202, −0.175, and −0.322 eV, respectively. Moreover, Table 1 shows the large equilibrium distances (more than 3.2 Å) and the small charge transfer (less than 0.1 e, absolute value) of these molecules. Clearly, the values of d_i are outside the length of the covalent radii of the C atom and Sn atom (2.15 Å), the O atom and Sn atom (2.22 Å), or the H atom and Sn atom (1.72 Å) [34,35]. It follows that these three types of gas molecules show the tendency for physisorption on the β-SnSe layer. However, for O_2 on the surface of the β-SnSe sheet, the optimized structure has a slight distortion. The E_a and Q_c are −1.596 and −0.445 eV, respectively, which are much larger than that of other gas molecules (CO, CO_2, CH_2O, NO_2, and SO_2) adsorbed on the β-SnSe monolayer. As for the d_i for O_2, it is 2.058 Å, which is within the length of the covalent radii of the O atom and Sn atom (2.22 Å) [35]. From this is can be concluded that the O_2 molecules are chemisorbed on the β-SnSe. When it comes to the adsorption properties of polluting gas molecules (e.g., NO_2 and SO_2) on the surface of β-SnSe, the E_a values are −0.829 and −0.499 eV, respectively, which are larger than the E_a of the molecules on the antimonene [14]. For NO_2 on the surface of GeS and α-SnSe monolayers, the values of E_a are −0.519 [11] and −0.770 eV [25], respectively, meaning that the adsorption behaviors of NO_2 and SO_2 molecules on β-SnSe are stronger than the aforementioned adsorption system. In addition, the charge transfer values for NO_2 and SO_2 are −0.279 and −0.278 eV, respectively, indicating that the charge transfer clearly happens between the gas molecules and the β-SnSe layer. The adsorption distance values for NO_2 and SO_2 are 2.531 Å and 2.692 Å, respectively, which is approaching the range of the Sn–O bond lengths (2.22 Å to 2.66 Å) [35]. It is of great significance for the β-SnSe sheet to detect NO_2 and SO_2 in the field of gas sensors. It is worth mentioning that all the most energetically stable adsorption sites are on the Sn atom's side of the β-SnSe sheet, showing that the adsorption properties of metal atoms are stronger than that of non-metal atoms [36].

Furthermore, the first principles molecular dynamics (MD) simulation lasted 5 ps with a step of 1 fs and the canonical ensemble (NVT) was applied at 300 K to examine the structural stability of a pristine β-SnSe sheet. Judging from Figure S1 (in the Supplementary Materials), results show that the total potential energy of a pristine β-SnSe sheet fluctuates a small amount before 2500 fs, and then keeps stable during the remaining 2500 fs. As for the structure of a pristine β-SnSe sheet, it has a slight deformation. This all shows that a pristine β-SnSe sheet is stable at 300 K.

Table 1. The adsorption properties (adsorption energy (E_a), Hirshfeld charge transfer (Q_c), and equilibrium distance (d_i)) of CO, CO_2, CH_2O, O_2, NO_2, and SO_2 on a β-SnSe monolayer.

Gas Molecule	E_a (eV)	Q_c (e)	d_i (Å)	Most Stable Site
CO	−0.202	−0.033	3.293 (C−Sn)	T_3
CO_2	−0.175	−0.036	3.617 (C−Sn)	T_3
CH_2O	−0.322	−0.085	3.222 (H−Sn)	T_2
O_2	−1.596	−0.445	2.058 (O−Sn)	T_2
NO_2	−0.829	−0.279	2.531 (O−Sn)	T_3
SO_2	−0.499	−0.278	2.692 (O−Sn)	T_2

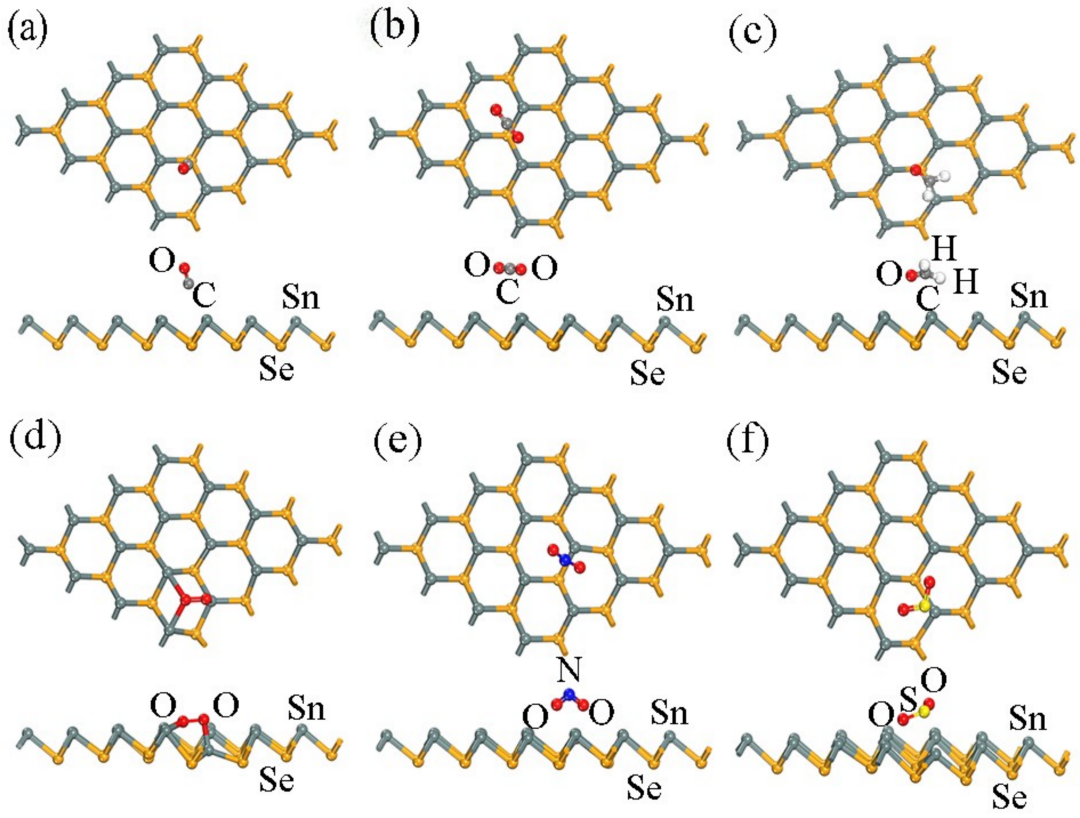

Figure 2. The most stable sites of optimized configurations of the adsorbate molecules: (**a**) CO, (**b**) CO_2, (**c**) CH_2O, (**d**) O_2, (**e**) NO_2, and (**f**) SO_2 adsorbed on a β-SnSe monolayer. The most stable sites are exhibited.

For the purpose of fully understanding the adsorption mechanism of the molecule-substrate systems, Figure 3 shows the calculation results of the density of states (DOSs) of the β-SnSe monolayer, molecule-SnSe systems, and the projected DOS for the adsorbate gas molecules. In addition, the band information of the molecule-substrate systems is plotted in Figure 4. Clearly, the summits of the DOSs of CO and CO_2 molecules illustrated in Figure 3a,b mainly localize below −3 eV in the valence band (VB), which are doubtless out of the Fermi level (E_f). In addition, judging from the band structure of the adsorption system, it is found that there is a slight influence on the band structure of the β-SnSe sheet. All of this indicates that CO and CO_2 are weakly adsorbed on the β-SnSe layer. As for the adsorption performances of CH_2O adsorbed on the β-SnSe sheet, the influences of the electronic levels of CH_2O molecules to the β-SnSe monolayer are mainly located in the interval ranging from −1.5 to −0.5 eV in the VB, which is not at the position of E_f. Thus, the changes in the band gaps and band structures are slight. In regard to the O_2 and SO_2 adsorbed on the surface of the β-SnSe sheet, it is found that these two gas molecules contribute the electronic levels of the adsorption system from −2.0 to 2.0 eV, which are close to the E_f. Accordingly, the band gap values of the molecule-substrate systems

of O_2 and SO_2 are 1.496 and 1.473 eV, respectively, revealing that the O_2 and SO_2 molecules have a strong influence on the electronic properties of the β-SnSe sheet. In terms of the electronic density of the state of NO_2 on β-SnSe, the peaks of NO_2, SnSe, and NO_2–SnSe gather and overlap near the E_f. In addition, the band structures of β-SnSe induce great changes with the appearance of NO_2 on the β-SnSe sheet. Thus, it is inferred that the existence of NO_2 has a dramatic influence on the electronic properties of the β-SnSe monolayer.

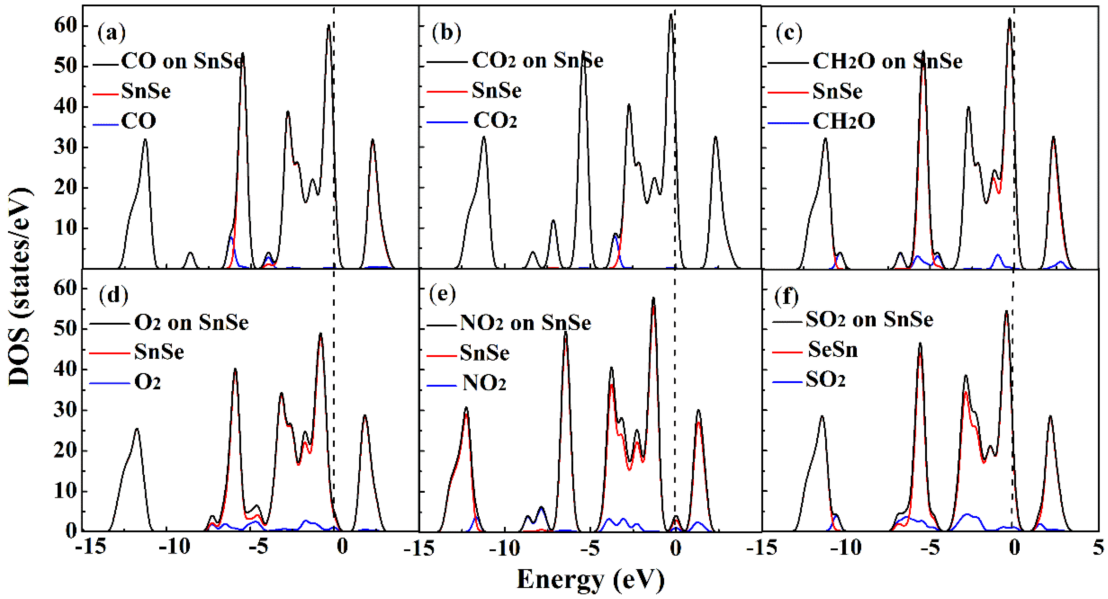

Figure 3. Total DOSs of the (**a**) CO, (**b**) CO_2, (**c**) CH_2O, (**d**) O_2, (**e**) NO_2 and (**f**) SO_2 on SnSe (black curve), the projected DOS of SnSe (red curve), and the adsorbate molecules (blue curve) for CO, CO_2, CH_2O, O_2, NO_2, SO_2 on SnSe monolayer. The E_f is set to zero, as illustrated by the black dotted line.

Furthermore, the slices of charge densities are presented in Figure 5. Using the slice of charge densities for the molecule-substrate systems, the electric distribution of the systems were investigated. Judging from Figure 5a–c, there are clearly no charges gathering between the atom in the gas molecule and the Sn atom. As for the charge density slices of O_2, NO_2, and SO_2, the high electronic densities are presented in the areas between the O atom and the Sn atom, see Figure 5d–f, indicating the emergence of covalent bonding in the molecule-substrate systems. In addition, the total charge carrier in the substrate can be changed via charge transfer, so the electronic properties of the substrate will be altered after the molecules are adsorbed on it [37,38]. Thus, it is of vital significance for β-SnSe to be applied in the field of gas sensors.

In addition, taking the effect of humidity on the substance into consideration, the adsorption performances of H_2O adsorbed on the β-SnSe sheet are calculated by first principles calculation. The most stable site of structural optimizations for H_2O on the β-SnSe layer is presented (see Figure S2 in the Supplementary Materials) The E_a, Q_c, and d_i of H_2O adsorbed on β-SnSe monolayer are −0.4038 eV, −0.0577 e, and 2.898 Å, respectively. The E_a and Q_c are small, the value of d_i is outside of the length of the covalent radii of the O atom and Sn atom (2.22 Å). The band gap value of the H_2O-substrate system is 1.962 eV, which is shown in Figure S3 (in the Supplementary Materials). The change in value of the band gap is small (0.012 eV). In addition, the peak of DOSs of the H_2O molecule illustrated in Figure S4 (in the Supplementary Materials) mainly localize below −2.5 eV in the valence band (VB), which are doubtless out of the Fermi level (E_f). Judging from Figure S5 (in the Supplementary Materials), there are clearly no charge distributions between the atom in the gas molecule and the Sn atom. All results show that H_2O has little effect on the β-SnSe monolayer.

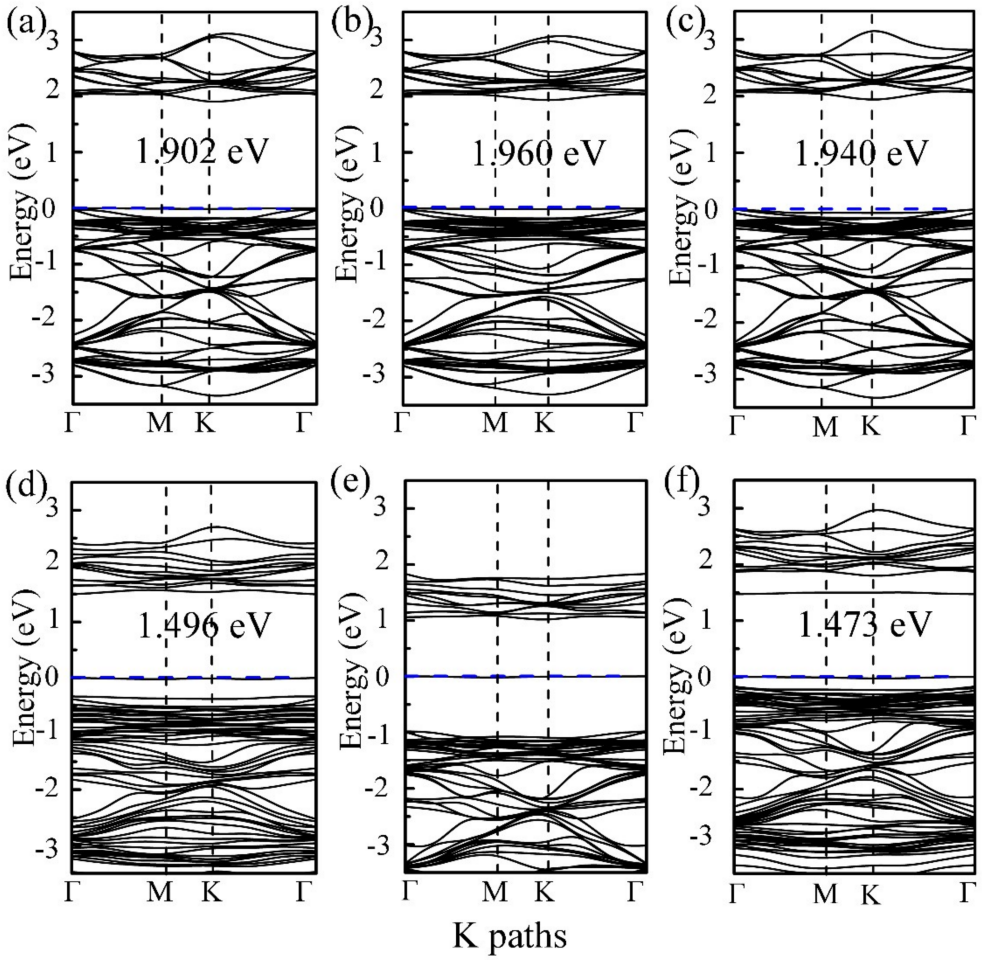

Figure 4. Band structures of the monolayered β-SnSe with the adsorbate molecules: (**a**) CO, (**b**) CO_2, (**c**) CH_2O, (**d**) O_2, (**e**) NO_2, and (**f**) SO_2, respectively. The E_f is set to zero, as presented via the blue dotted line.

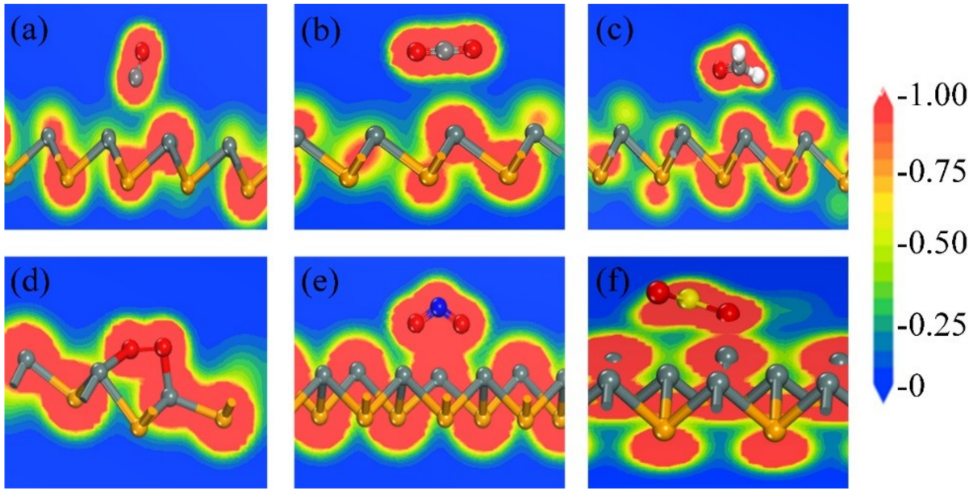

Figure 5. The slice of charge densities for the β-SnSe monolayer with the adsorbate molecules: (**a**) CO, (**b**) CO_2, (**c**) CH_2O, (**d**) O_2, (**e**) NO_2, and (**f**) SO_2, respectively. The value of electron densities ranges between 0 and 1.00 e/Å^3.

4. Conclusions

In summary, the adsorption and electronic characteristics of a β-SnSe monolayer for CO, CO_2, CH_2O, O_2, NO_2, and SO_2 have been carried out by first principles calculation. The CO, CO_2, and CH_2O can be physisorbed on the β-SnSe monolayer. Because the adsorptions of CH_2O on the β-SnSe monolayer have relatively numerous charge transfers and a significant effect on the DOS, it is deduced that the β-SnSe layer can be employed to detect CH_2O. In addition, O_2, NO_2, and SO_2, show strong adsorption energy, charge transfer, and dramatic changes to the electronic properties, meanwhile, covalent bonds are formed between the O atom and the Sn atom. Thus, they are chemisorbed on the β-SnSe monolayer, suggesting that the β-SnSe monolayer can be employed to detect and catalyze these three types of gas molecules.

Supplementary Materials: The following are available online at http://www.mdpi.com/2079-6412/9/6/390/s1, Figure S1: Total potential energy of pristine monolayer SnSe at 300 K within 5 ps during the first-principles molecular dynamics (MD) simulation; Figure S2: The most stable site of structural optimizations for H_2O on β-SnSe layer is presented; Figure S3: Band structure of the monolayered β-SnSe with the H_2O molecules; Figure S4: Total DOSs of the H_2O on SnSe (black curve), the projected DOS of SnSe (red curve), and the adsorbate molecules (blue curve) for H_2O on SnSe monolayer. The E_f is set to zero, as illustrated by black dotted line; Figure S5: The slice of charge densities for the β-SnSe monolayer with the H_2O molecule. The value of electron densities ranges between 0 and 1.00 e/Å^3.

Author Contributions: Conceptualization, H.Q. and T.L.; Methodology, H.Q. and T.L.; Software, T.L. and H.Q.; Validation, T.L.; Formal Analysis, T.L.; Investigation, T.L. and H.Q.; Resources, T.L.; Data Curation, T.L.; Writing—Original Draft Preparation, H.Q. and T.L.; Writing—Review and Editing, D.Y. and G.Z.; Visualization, T.L.; Supervision, H.Q. and D.Y.; Project Administration, H.Q.; Funding Acquisition, H.Q. All authors read and approved the final manuscript.

Funding: Our investigation was supported by the project of Natural Science Foundation of Guangxi Zhuang Autonomous Region (grant No. 2016GXNSFBA380114), and Innovation Project of GUET Graduate Education (grant No. 2018YJCX04).

Acknowledgments: The authors gratefully acknowledge the financial supports by the Natural Science Foundation of Guangxi Zhuang Autonomous Region (grant No. 2016GXNSFBA380114), and Innovation Project of GUET Graduate Education (grant No. 2018YJCX04).

Conflicts of Interest: The authors declare that the work described was original research that has not been published previously, and is not under consideration for publication elsewhere, in whole or in part. All the authors listed have approved the final manuscript.

References

1. Kong, J.; Franklin, N.R.; Zhou, C.; Chapline, M.G.; Peng, S.; Cho, K.; Dai, H. Nanotube molecular wires as chemical sensors. *Science* **2000**, *287*, 622–625. [CrossRef] [PubMed]
2. Penza, M.; Martucci, C.; Cassano, G. NO_x gas sensing characteristics of WO_3 thin films activated by noble metals (Pd, Pt, Au) layers. *Sens. Actuator B Chem.* **1998**, *50*, 52–59. [CrossRef]
3. Choi, S.J.; Jang, B.H.; Lee, S.J.; Min, B.K.; Rothschild, A.; Kim, I.D. Selective detection of acetone and hydrogen sulfide for the diagnosis of diabetes and halitosis using SnO_2 nanofibers functionalized with reduced graphene oxide nanosheets. *ACS Appl. Mater. Inter.* **2015**, *6*, 2588–2597. [CrossRef] [PubMed]
4. Yang, W.; Gan, L.; Li, H.; Zhai, T. Two-dimensional layered nanomaterials for gas-sensing applications. *Inorg. Chem. Fron.* **2016**, *3*, 433–451. [CrossRef]
5. Luo, H.C.; Meng, R.S.; Gao, H.; Sun, X.; Xiao, J.; Ye, H.Y.; Zhang, G.Q.; Chen, X.P. First-principles study of nitric oxide sensor based on blue phosphorus monolayer. *IEEE Electron Device Lett.* **2017**, *38*, 1139–1142. [CrossRef]
6. Yuan, W.; Shi, G. Graphene-based gas sensors. *J. Mater. Chem. A* **2013**, *1*, 10078–10091. [CrossRef]
7. Zhang, S.; Yan, Z.; Li, Y.; Chen, Z.; Zeng, H. Atomically thin arsenene and antimonene: semimetal-semiconductor and indirect-direct band-gap transitions. *Angew. Chem.* **2015**, *54*, 3112–3115. [CrossRef]
8. Tan, C.; Cao, X.; Wu, X.J.; He, Q.; Yang, J.; Zhang, X.; Chen, J.; Zhao, W.; Han, S.; Nam, G.H.; et al. Recent advances in ultrathin two-dimensional nanomaterials. *Chem. Rev.* **2017**, *117*, 6225–6331. [CrossRef]

9. Varghese, S.; Varghese, S.; Swaminathan, S.; Singh, K.; Mittal, V. Two-dimensional materials for sensing: graphene and beyond. *Electronics* **2015**, *4*, 651–687. [CrossRef]
10. Yang, S.; Jiang, C.; Wei, S.-H. Gas sensing in 2D materials. *Appl. Phys. Rev.* **2017**, *4*, 021304. [CrossRef]
11. Wang, S.G.; Tan, C.J.; Yang, Q.; Xu, Y.X.; Li, S.L.; Chen, X.P. A novel ultra-sensitive nitrogen dioxide sensor based on germanium monosulfide monolayer. *IEEE Electron Device Lett.* **2017**, 1590–1593. [CrossRef]
12. Chen, C.W.; Hung, S.C.; Yang, M.D.; Yeh, C.W.; Wu, C.H.; Chi, G.C.; Ren, F.; Pearton, S.J. Oxygen sensors made by monolayer graphene under room temperature. *Appl. Phys. Lett.* **2011**, *99*, 243502. [CrossRef]
13. Das, S.; Pandey, D.; Thomas, J.; Roy, T. The role of graphene and other 2D materials in solar photovoltaics. *Adv. Mater.* **2019**, *31*, e1802722. [CrossRef]
14. Meng, R.S.; Cai, M.; Jiang, J.K.; Liang, Q.H.; Sun, X.; Yang, Q.; Tan, C.J.; Chen, X.P. First principles investigation of small molecules adsorption on antimonene. *IEEE Electron Device Lett.* **2017**, *38*, 134–137. [CrossRef]
15. Haq, B.U.; Alfaify, S.; Ahmed, R.; Butt, F.K.; Shkir, M. Exploring single-layered SnSe honeycomb polymorphs for optoelectronic and photovoltaic applications. *Phys. Rev. B* **2018**, *97*, 075438. [CrossRef]
16. Tao, L.; Cinquanta, E.; Chiappe, D.; Grazianetti, C.; Fanciulli, M.; Dubey, M.; Molle, A.; Akinwande, D. Silicene field-effect transistors operating at room temperature. *Nat. Nanotechnol.* **2015**, *10*, 227–231. [CrossRef] [PubMed]
17. Gillgren, N.; Wickramaratne, D.; Shi, Y.; Espiritu, T.; Yang, J.; Hu, J.; Wei, J.; Liu, X.; Mao, Z.; Watanabe, K.; et al. Gate tunable quantum oscillations in air-stable and high mobility few-layer phosphorene heterostructures. *2D Mater.* **2014**, *2*, 011001. [CrossRef]
18. Khan, M.A.H.; Rao, M.V.; Li, Q. Recent advances in electrochemical sensors for detecting toxic gases: NO_2, SO_2 and H_2S. *Sensors* **2019**, *19*, 905. [CrossRef]
19. Zheng, K.; Yang, Q.; Tan, C.J.; Ye, H.Y.; Chen, X.P. A two-dimensional van der Waals CdS/germanene heterojunction with promising electronic and optoelectronic properties: DFT + NEGF investigations. *Phys. Chem. Chem. Phys.* **2017**, *19*, 18330–18337. [CrossRef]
20. Tang, C.; Li, Q.; Zhang, C.; He, C.; Li, J.; Ouyang, T.; Li, H.; Zhong, J. Stability and magnetic properties of SnSe monolayer doped by transition metal atom (Mn, Fe, and Co): A first-principles study. *J. Phys. D. Appl. Phys.* **2018**, *51*, 245004. [CrossRef]
21. Patil, S.G.; Tredgold, R.H. Electrical and photoconductive properties of SnS2 crystals. *J. Phys. D. Appl. Phys.* **1971**, *4*, 718–722. [CrossRef]
22. Minnam Reddy, V.R.; Gedi, S.; Pejjai, B.; Park, C. Perspectives on SnSe-based thin film solar cells: A comprehensive review. *J. Mater. Sci. Mater. Electron.* **2016**, *27*, 5491–5508. [CrossRef]
23. Nabi, Z.; Kellou, A.; Méçabih, S.; Khalfi, A.; Benosman, N. Opto-electronic properties of rutile SnO_2 and orthorhombic SnS and SnSe compounds. *Mater. Sci. Eng. B* **2003**, *98*, 104–115. [CrossRef]
24. Hu, F.-F.; Tang, H.-Y.; Tan, C.-J.; Ye, H.-Y.; Chen, X.-P.; Zhang, G.-Q. Nitrogen dioxide gas sensor based on monolayer SnS: A first-principle study. *IEEE Electron Device Lett.* **2017**, *38*, 983–986. [CrossRef]
25. Wang, J.; Yang, G.F.; Xue, J.J.; Lei, J.M.; Chen, D.J.; Lu, H.; Zhang, R.; Zheng, Y.D. A reusable and high sensitivity nitrogen dioxide sensor based on monolayer SnSe. *IEEE Electron Device Lett.* **2018**, 718–722. [CrossRef]
26. Hu, Z.Y.; Li, K.Y.; Lu, Y.; Huang, Y.; Shao, X.H. High thermoelectric performances of monolayer SnSe allotropes. *Nanoscale* **2017**, *9*, 16093–16100. [CrossRef] [PubMed]
27. Kohn, W.; Sham, L.J. Self-consistent equations including exchange and correlation effects. *Phys. Rev.* **1965**, *140*, A1133–A1138. [CrossRef]
28. Perdew, J.P.; Burke, K.; Ernzerhof, M. Generalized gradient approximation made simple. *Phys. Rev. Lett.* **1997**, *78*, 1396–1396. [CrossRef]
29. Yu, D.; Li, M.; Yu, T.; Wang, C.; Zeng, Y.; Hu, X.; Chen, G.; Yang, G.; Du, F. Nanotube-assembled pine-needle-like CuS as an effective energy booster for sodium-ion storage. *J. Mater. Chem. A* **2019**, *7*, 10619–10628. [CrossRef]
30. Stefan, G. Semiempirical GGA-type density functional constructed with a long-range dispersion correction. *J. Comput. Chem.* **2010**, *27*, 1787–1799.
31. Andzelm, J.; Govind, N.; Fitzgerald, G.; Maiti, A. DFT study of methanol conversion to hydrocarbons in a zeolite catalyst. *Int. J. Quantum Chem.* **2003**, *91*, 467–473. [CrossRef]
32. Pan, X.; Cai, Q.X.; Chen, W.L.; Zhuang, G.L.; Li, X.N.; Wang, J.G. A DFT study of gas molecules adsorption on the anatase (001) nanotube arrays. *Comp. Mater. Sci.* **2013**, *67*, 174–181. [CrossRef]

33. Zhao, J.Y.; Zhao, F.Q.; Ju, X.H.; Gao, H.X.; Zhou, S.Q. Density functional theory studies on the adsorption of NH_2NO_2 on Al_{13} Cluster. *J. Clust. Sci.* **2012**, *23*, 395–410. [CrossRef]
34. Pyykko, P.; Atsumi, M. Molecular single-bond covalent radii for elements 1-118. *Chemistry* **2009**, *15*, 186–197. [CrossRef] [PubMed]
35. Brown, I.D. Bond valence as an aid to understanding the stereochemistry of O and F complexes of Sn(II), Sb(III), Te(IV), I(V) and Xe(VI). *J. Solid State Chem.* **1974**, *11*, 214–233. [CrossRef]
36. Feng, C.; Qin, H.; Yang, D.; Zhang, G. First-principles investigation of the adsorption behaviors of CH_2O on BN, AlN, GaN, InN, BP, and P monolayers. *Materials* **2019**, *12*, 676. [CrossRef] [PubMed]
37. Feng, C.; Qin, H.; Luan, X.; Kuang, T.; Yang, D. Gas sensing properties of two-dimensional penta-BP 5: A first-principles study. *Chem. Phys. Lett.* **2018**, *706*, 355–359. [CrossRef]
38. Cho, B.; Hahm, M.G.; Choi, M.; Yoon, J.; Kim, A.R.; Lee, Y.J.; Park, S.G.; Kwon, J.D.; Kim, C.S.; Song, M.; et al. Charge-transfer-based gas sensing using atomic-layer MoS2. *Sci. Rep. UK* **2015**, *5*, 8052. [CrossRef]